Laura Zulian*, Francesco Segrado and Dario Narducci

Effect of the Annealing on the Low-Temperature Charge Transport Properties of Heavily Boron-Doped Nanocrystalline Silicon Films for Thermoelectric Applications

DOI 10.1515/ehs-2016-0012

Abstract: Silicon is the reference material of microelectronics, is readily available, relatively unexpensive, and its use may take profit of a fantastic technology. This may explain why a substantial effort has focused on improving its thermoelectric efficiency, either by top-down nanostructuring or through suitable processing. In this paper we report an analysis of the electronic transport properties of heavily boron-doped nanocrystalline silicon films. High-temperature thermal treatments are confirmed to remarkably increase its thermoelectric power factor. Electrical conductivity and Hall effect measurements were carried out over the temperature range 20–300 K along with Seebeck coefficient measurements. We provide evidence of the occurrence of low-temperature hopping conduction between impurity subbands. Dopant ionization was studied as a function of temperature. Freeze-out temperature was found to correlate with the Seebeck coefficient in agreement with Pisarenko equation. This brings to the conclusion that, while untreated samples are weakly degenerate, the thermal processing reverts them into non-degenerate semiconductors, in spite of the high doping level.

Keywords: silicon, annealing, energy filtering, thermoelectricity, microharvesting

1 Introduction

The need and the opportunity of converting low enthalpy heat into electricity using thermoelectric generators has motivated over the last decade an impressive surge of material research worldwide. On one side, *macro*harvesting, i. e. the recover of waste heat from industrial plants, homes, or car mufflers may help reduce the use of non–renewable primary energy sources, still today mostly of fossil origin, while favorably impacting on greenhouse gas emissions. On the other side, *micro*harvesting is believed to be one of the most interesting power sources to enable wireless sensor networks, replacing batteries.

To this aim, however, novel thermoelectric materials are needed, since the current standards, based upon tellurium, could never cover the anticipated market requests in both macro and microharvesting due to raw material scarcity. In this respect, silicon and silicon–based thermoelectric materials would be game-changers, not only because of silicon geo-abundance but also because of the ease of integrating thermoelectric silicon with microelectronic components and circuits.

Rather unfortunately, single-crystalline silicon is a quite poor thermoelectric material, with a low thermoelectric figure of merit (≈ 0.01). Actually, while its power factor $\sigma\alpha^2$ (where σ is the electrical conductivity and α is the Seebeck coefficient) may be relatively large, its thermal conductivity κ is >100 W/mK. Strategies to decrease κ in single crystals by selective scattering of phonons in one–dimensional nanostructures have demonstrated very effective (Hochbaum et al. 2008; Boukai et al. 2008), leading to figures of merit $ZT = \sigma\alpha^2 T/\kappa \approx 0.8$ at temperature T around 300 K. This is however not the only possible approach, as comparable ZT have been shown to be achievable in nanocrystalline silicon, where κ is reduced by phonon scattering at grain boundaries. It could be shown (Narducci et al. 2012, 2014) that proper annealing of the material may fully compensate for the reduction of electrical conductivity due to polycrystallinity through hole energy filtering (Narducci, Frabboni, and Zianni 2015).

While the physics of energy filtering itself is fairly well understood (Bahk, Bian, and Shakouri 2013; Neophytou et al. 2013; Zianni and Narducci 2015), the details of the chemical process leading to the formation of potential barriers at grain boundaries is still to be elucidated. Thus, a research endeavor has been undertaken to correlate annealing cycles, boron distribution,

***Corresponding author: Laura Zulian,** Dept. of Materials Science, University of Milano Bicocca, Via Roberto Cozzi 55, Milano 20126, Italy, E-mail: laura.zulian@gmail.com

Francesco Segrado, Dario Narducci, Dept. of Materials Science, University of Milano Bicocca, Via Roberto Cozzi 55, Milano 20126, Italy

and transport properties in nanocrystalline silicon thin films. This paper focuses on understanding the correlation between thermal treatments and the electronic structure of nanosilicon films, using material transport properties as a probe. By comparing untreated and thermally treated films it will be shown that *any* prolonged thermal process at >900 °C leads to one, possibly unexpected, effect – that of converting degenerate nanosilicon back into a non–degenerate semiconductor.

2 Experimental Procedure

Nanocrystalline Si films were grown by chemical vapor deposition (CVD) at 610 °C onto oxidized (100) silicon wafers. Film thickness was measured to be 228 ± 5 nm. Silicon was boron–doped by ion implantation (26 keV, 6×10^{15} cm^{-2} + 47 keV, 6×10^{15} cm^{-2}) followed by rapid thermal processing (1,050 °C, 20 s) to a total nominal boron density of 4.4×10^{20} cm^{-3}. Samples were cut from the wafer and then eventually submitted to additional thermal treatments in argon (Table 1). Prior to annealing them, samples were submitted to Piranha etch (H_2SO_4 96 % vol.:H_2O_2 30 % vol. = 2:1, 95 °C, 30 min) to remove organic surface contaminants, then rinsed in ultrapure deionized water, and dried under nitrogen flux. Oxide was removed by DHF (HF 40 % vol.:H_2O = 1:10) up to obtaining a fully hydrophobic surface, then the specimen was rinsed in ultrapure deionized water, and finally dried under nitrogen flux. For double thermal treatments, an additional DHF etching was carried out between the two annealing steps to remove oxidized layers that might have formed.

Table 1: Processing and physical properties of the samples studied in this work. Carrier density p and Seebeck coefficient α refer to 300 K.

Sample	Processing	T_{out} (K)	T_{in} (K)	ε_h (meV)	α(300 K) (mV/K)	p(300 K) (cm^{-3})
A	900 °C, 2 h	110	45	0.007	0.41	7.0×10^{19}
B	1,000 °C, 2 h	90	40	0.15	0.47	8.4×10^{19}
C	900 °C, 2 h + 1,000 °C, 2 h	80	40	0.16	0.62	5.5×10^{19}
D	1,000 °C, 2 h + 1,000 °C, 2 h	72	53	0.13	0.67	6.3×10^{19}
E	1,000 °C, 4 h	85	30	0.09	0.47	6.2×10^{19}

Electrical resistivity, Hall resistance, and Seebeck coefficient were measured. Aluminum contact evaporation was carried out after removing eventual oxide layers by DHF. Contact characteristics were verified to be always linear.

Seebeck coefficients were measured at 300 K using the integral method. Each measurement was carried out in triplicate to assess its reproducibility. Hall resistivity R_H was measured between 20 and 300 K with a maximum magnetic field of 0.5 T. Electrical conductivity was obtained as a function of temperature between 20 and 300 K extracting it from four–probe current–voltage characteristics. Further details on the experimental procedure were reported elsewhere (Zulian, Segrado, and Narducci 2017).

3 Results and Discussion

The temperature dependencies of σ and R_H were preliminary analyzed in a previous publication (Zulian, Segrado, and Narducci 2017). Thus, they will be only summarized hereafter.

Inspection of experimental data immediately shows the remarkable qualitative difference between the untreated (non annealed) film on one side; and *all* the heat–treated films on the other side. Actually, the untreated sample displays a monotonic increase of σ as T decreases, with the carrier density being almost constant from 20 K up to 300 K (Figure 1, top). Instead, in all annealed samples σ reaches a

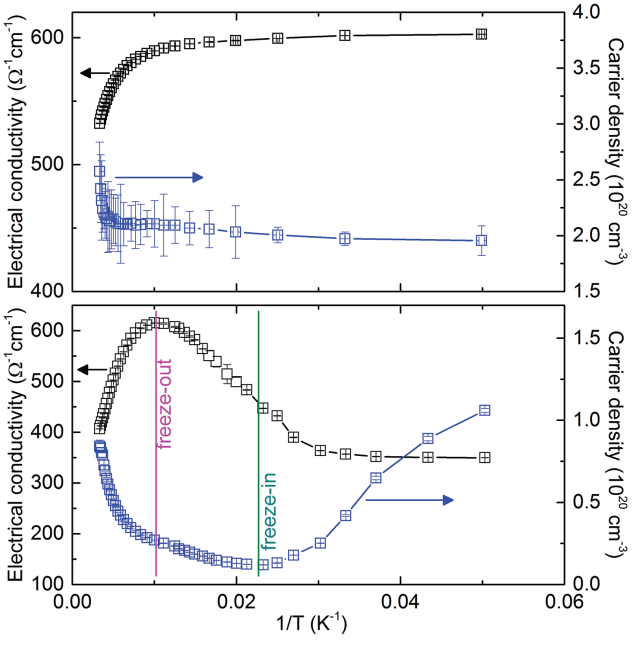

Figure 1: Comparative trend of the electrical conductivity and of the carrier density vs. the reciprocal temperature in untreated (top) and heat–treated (bottom) samples. While the former shows a typical metal–like behavior, heat treatments leads to non-monotonic $p(T)$ and $\sigma(T)$ curves. Freeze–out temperature T_{out} marks the maximum of σ and a saddle point of p while the freeze–in temperature T_{in} is displayed as a minimum for the carrier density.

maximum, then decreases getting to an asymptotic value in the zero-temperature limit (Figure 1, bottom).

For the untreated sample it is quite immediate to conclude that the large boron doping brings silicon beyond the degeneracy threshold. The impurity band due to acceptor interactions overlaps with the valence band. Continuity of electronic states leads to a quasi–metallic electronic structure (weak degeneracy) (Blackemore 2002) so that the carrier density remains constant when raising the temperature while the conductivity slowly drops with it due to electron–phonon scattering.

This standard picture does not apply instead to the heat–treated samples. The trend that is observed may however be explained as follows (Hung and Gliessman 1954). In the low temperature limit acceptors contribute to charge transport only by hopping. As temperature raises an increasingly large number of centers gets ionized, leading to an increasing carrier density for band transport up to a temperature at which all centers are ionized. This causes an increase of σ. For higher temperature no additional carriers can be made available, save for those generated by interband transitions. Therefore conductivity is dominated by the mobility decrease due to the augmented phonon–electron scattering rate. Two critical temperatures may be then defined, namely

1. a freeze–out temperature T_{out} at which all acceptors are ionized, so that the conductivity gets to a maximum;
2. a freeze–in temperature T_{in}, at which acceptor ionization is virtually zero.

A signature of the two temperatures is expected to be displayed by both $\sigma(T)$ and $p(T)$. The clearest mark of T_{out} is obviously set by the maximum of σ. However, also $p(T)$ reports it. Actually, since at T_{out} all acceptors are ionized, at such temperature the carrier density p should display a plateau, eventually followed by a new increase at higher temperatures, where intrinsic carriers begin contributing to hole density. This is actually the case in lightly doped semiconductors (Luryi, Shklovskii, and Efros 2013). Instead, in heavily doped silicon the plateau reduces to a saddle point. As of T_{in}, since competition between delocalized (band) and hopping carriers occurs when all acceptors are frozen in their neutral state, T_{in} is the temperature at which carrier density $p(T)$ gets to its minimum. Figure 1 displays both critical temperatures with reference to a typical annealed sample.

This analysis is corroborated by the comparison of the electrical conductivity in the low and high temperature limits. In general, both hopping and band conduction contribute to σ as (Hung 1950)

$$\sigma = e\mu_h p_h + e\mu_b p_b \quad [1]$$

where the subscripts label hopping (h) and band (b) terms. Likewise, the Hall resistance reads

$$R_H = r\frac{e\mu_h^2 p_h + e\mu_b^2 p_b}{(e\mu_h p_h + e\mu_b p_b)^2} \quad [2]$$

where r is a constant of the order of unity. Thus, in the low-temperature limit $p_b \cong 0$ and then $p_h \cong p$ so that $R_H \cong r/(ep_h) \cong r/(ep)$. Instead in the high temperature limit $p_h \cong 0$ and $p_b \cong p$ so that $R_H \cong r/(ep_b) \cong r/(ep)$. Thus, the two limiting Hall resistivities are predicted to be equal to each other. This was actually shown to be the case in all annealed samples (Chroboczek, Pollak, and Staunton 1984; Zulian, Segrado, and Narducci 2017).

Carrier freeze–out provides additional information concerning the density of states (DOS) in the samples. Interactions among acceptor states in heavily doped nanocrystalline semiconductors lead to the formation of an impurity band that may eventually overlap with the valence band. In a simplistic view, boron levels open up to form an impurity band centered at the isolated acceptor energy E_A (measured from the top of the valence band) with a width (Schubert 2015)

$$\delta E = \frac{e^2}{4\pi\varepsilon p^{-1/3}} \quad [3]$$

where ε is the semiconductor permittivity. Thus, overlap starts occurring for a critical acceptor density

$$p_c = \left(\frac{4\pi\varepsilon E_A}{e^2\sqrt{\log 2}}\right)^3 \quad [4]$$

In silicon this sets $p_c \cong 9\times10^{19}$ cm^{-3}, namely about a fifth of the nominal boron concentration of the present samples. Whenever a significant band overlap occurs, however, no freeze–out should be observed since the Fermi level would sweep a continuum of states. Actually, carrier density in all samples is lower than p_c at room temperature (Table 1), being obviously even lower at lower temperatures – confirming that a relevant part of boron impurities cluster and precipitate within silicon (Narducci et al. 2012, 2014).

Although this picture properly describes the band conduction, a more accurate description of the impurity band is needed to explain the low temperature carrier transport. Should one simply take the acceptor levels to provide a single impurity band, a hopping activation energy ε_h comparable to E_A would be expected, in blatant contrast with observations. Actually, in heavily doped silicon the electrostatic interactions lead to the formation of three

sub-bands, $A^{(0)}$, $A^{(-)}$, and $A^{(+)}$ (this being formally a donor sub-band), depending on the charge state of the impurity itself. Computations (Poklonskii and Syaglo 1999) predict a band split $E_{A^{(+)}} - E_{A^{(0)}}$ of ≈ 5 meV at an acceptor density $N_A \approx 10^{17} - 10^{18}$ cm^{-3}. Since the separation between the $A^{(0)}$ and the $A^{(+)}$ sub-bands is also the activation energy for the hopping transport, we may estimate that at carrier densities in the order of 10^{20} cm^{-3} the sub–band split reduces to fractions of meV (Table 1). Thus, considering that, using eq. [3], the sub–band width may be estimated to be ≈ 38 meV, the convoluted impurity band can be predicted to display a non–monotonic dependency on the energy due to the sub-band overlap.

Further insights in the electronic structure of the material come from the analysis of the Seebeck coefficient. Figure 2 displays the dependence of α upon $1/T_{out}$. It is to be noted that T_{out} increases with the doping level (Figure 3), as at larger impurity contents a higher temperature is needed for all dopant levels to be ionized. Stated differently, silicon must be set to a higher temperature for the overall carrier density (as resulting from both extrinsic and intrinsic contributions) to equal the dopant density. One may actually verify that $\ln N_A \propto 1/T_{out}$. Thus, also the Seebeck coefficient should decrease with T_{out}, as actually observed. As however α is approximately proportional to $1/T_{out}$, one may also conclude that Mott's formula for metals and semi-metals,

$$\alpha = \frac{8\pi^2 k_B^2}{3eh^2} m^* T \left(\frac{\pi}{3p}\right)^{2/3} \qquad [5]$$

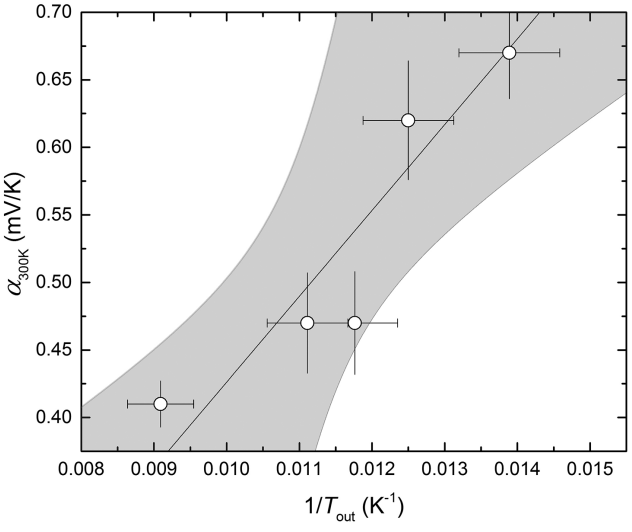

Figure 2: Relationship between the Seebeck coefficient at 300 K and the experimental freeze–out temperature. Confidence bands are at 95 %.

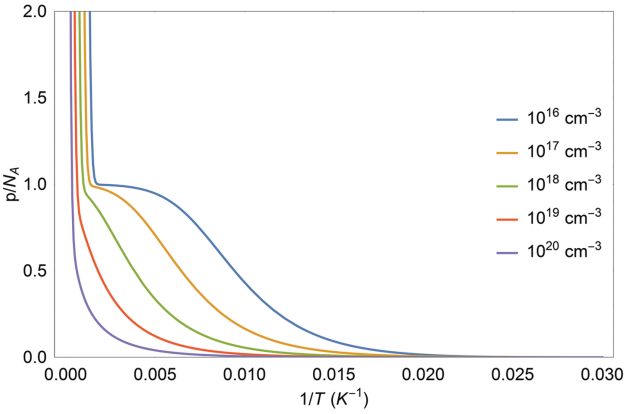

Figure 3: Ratio between the total carrier density and the impurity concentration in boron–doped silicon as a function of the reciprocal temperature at various doping levels.

(where k_B, h, and m^* are the Boltzmann constant, the Planck constant, and the effective mass of the majority carrier) although often invoked in the analysis of the Seebeck coefficient for heavily doped semiconductors (Ioffe 1957), is of no use in this case. Instead, Pisarenko equation

$$\alpha = \frac{k_B}{e}\left(\text{const.} + \ln\frac{2(2\pi m^* k_B T)^{3/2}}{h^3 p}\right) \qquad [6]$$

is apparently more consistent with the experiment, in spite of the high doping level.

On the basis of temperature dependencies of the carrier density and of the electrical conductivity, and of the just mentioned consistency of the experimental $\alpha(p)$ with the Pisarenko equation one may safely conclude that heat treatments succeed at removing the (weak) degeneracy of nanosilicon films observed in the untreated sample. It is sensible that such an effect is related to the precipitation of boron-enriched second phases at grain boundaries, that has been widely proved to be a necessary condition for ZT enhancement in nanosilicon (Narducci et al. 2012). The consequent reduction of the dissolved boron density, along with the relatively low solubility of boron into silicon (compared, e. g., to phosphorus), justifies the formation of a gap between the impurity (acceptor) band and the valence band, leading in turn to carrier freeze–out at temperatures around 100 K. Consistently, hopping conduction is observed at low temperatures.

4 Summary and Conclusions

In this paper we have analyzed the differences between the electronic transport properties of untreated and heat–treated heavily boron–doped nanosilicon films. It has

been shown that untreated samples are degenerate, reporting a quasi–metallic behavior. Instead, any long-term thermal treatment at >900 °C converts the degenerate nanosilicon back into a non–degenerate semiconductor. Full consistency of $p(T)$, $\sigma(T)$, and $\alpha(p)$ curves with this model has been discussed. Removal of degeneracy is also consistent with the experimentally assessed evidence that high-temperature annealing promote the diffusion–limited precipitation of boron at grain boundaries, enabling energy filtering of majority carriers and a favorable microscopic distribution of the temperature gradient within the material.

The availability of a model for the evolution of nanosilicon electronic structure enables a more detailed analysis of the quantitative differences among nanosilicon films experiencing single or repeated thermal processing. Such a comparative study will be the subject of a forthcoming publication.

Funding: This work was supported by FP7–NMP–2013–SMALL-7, SiNERGY (Silicon Friendly Materials and Device Solutions for Microenergy Applications) Project, Contract n. 604169.

References

Bahk, J. -H., Z. Bian, and A. Shakouri. 2013. "Electron Energy Filtering by a Nonplanar Potential to Enhance the Thermoelectric Power Factor in Bulk Materials." *Physical Review B* 87:075204.

Blackemore, J. 2002. *Semiconductor Statistics*. Mineola: Dover Publications.

Boukai, A. I., Y. Bunimovich, J. Tahir-Kheli, J. K. Yu, W. A. Goddard, and J. R. Heath. 2008. "Silicon Nanowires as Efficient Thermoelectric Materials." *Nature* 451:168–71.

Chroboczek, J., F. Pollak, and H. Staunton. 1984. "Impurity Conduction in Silicon and Effect of Uniaxial Compression on p-Type Si." *Philosophical Magazine Part B* 50:113–56.

Hochbaum, A. I., R. K. Chen, R. D. Delgado, W. J. Liang, E. C. Garnett, M. Najarian, A. Majumdar, and P. D. Yang. 2008. "Enhanced Thermoelectric Performance of Rough Silicon Nanowires." *Nature* 451:163–67.

Hung, C. 1950. "Theory of Resistivity and Hall Effect at Very Low Temperatures." *Physical Review* 79:727.

Hung, C., and J. Gliessman. 1954. "Resistivity and Hall Effect of Germanium at Low Temperatures." *Physical Review* 96:1226.

Ioffe, A. 1957. *Semiconductor Thermoelements and Thermoelectric Cooling*. London: Infosearch Ltd.

Luryi, S., B. Shklovskii, and A. Efros. 2013. *Electronic Properties of Doped Semiconductors*, Springer Series in Solid-State Sciences. Berlin Heidelberg: Springer.

Narducci, D., S. Frabboni, and X. Zianni. 2015. "Silicon De Novo: Energy Filtering and Enhanced Thermoelectric Performances of Nanocrystalline Silicon and Silicon Alloys." *Journal of Materials Chemistry C* 3:12176–85.

Narducci, D., B. Lorenzi, X. Zianni, N. Neophytou, S. Frabboni, G. C. Gazzadi, A. Roncaglia, and F. Suriano. 2014. "Enhancement of the Power Factor in Two-Phase Silicon-Boron Nanocrystalline Alloys." *Physica Status Solidi A* 211:1255–58.

Narducci, D., E. Selezneva, G. Cerofolini, S. Frabboni, and G. Ottaviani. 2012. "Impact of Energy Filtering and Carrier Localization on the Thermoelectric Properties of Granular Semiconductors." *Journal of Solid State Chemistry* 193:19–25.

Neophytou, N., X. Zianni, H. Kosina, S. Frabboni, B. Lorenzi, and D. Narducci. 2013. "Simultaneous Increase in Electrical Conductivity and Seebeck Coefficient in Highly Boron-Doped Nanocrystalline Si." *Nanotechnology* 24:205402.

Poklonskii, N., and A. Syaglo. 1999. "Electrostatic Model of the Energy Gap between Hubbard Bands for Boron Atoms in Silicon." *Semiconductors* 33:391–93.

Schubert, E. 2015. *Physical Foundations of Solid-State Devices*. Troy, NY: E. Fred Schubert.

Zianni, X., and D. Narducci. 2015. "Parametric Modeling of Energy Filtering by Energy Barriers in Thermoelectric Nanocomposites." *Journal of Applied Physics* 117:035102.

Zulian, L., F. Segrado, and D. Narducci. 2017. "Annealing of Heavily Boron-Doped Silicon: Effect on Electrical and Thermoelectric Properties." *Journal of Nanoscience and Nanotechnology* 17:1657–62.